PCCP

PAPER

View Article Online
View Journal | View Issue

Cite this: *Phys. Chem. Chem. Phys.*, 2014, **16**, 18282

Quasi-planar aromatic B_{36} and B_{36}^- clusters: all-boron analogues of coronene†

Qiang Chen,[a] Guang-Feng Wei,[b] Wen-Juan Tian,[a] Hui Bai,[a] Zhi-Pan Liu,[b] Hua-Jin Zhai*[ac] and Si-Dian Li*[a]

Received 10th May 2014,
Accepted 15th July 2014

DOI: 10.1039/c4cp02032d

www.rsc.org/pccp

Flat boron has recently emerged as a fascinating concept in cluster science. Here we present computational evidence for the quasi-planar all-boron aromatic B_{36} (C_{6v}, $^1A_1$) and B_{36}^- (C_{2v}, $^2A_1$) clusters, established as the global-minimum structures on the basis of Stochastic Surface Walking (SSW) searches. The energetics for low-lying isomeric structures are evaluated using the validated density-functional method at the PBE0/6-311+G* level. Our global-minimum structures are in line with a recent report (Z. A. Piazza *et al.*, *Nat. Commun.*, 2014, **5**, 3113). These structures consist of two-dimensional close-packing boron with a perfect hexagonal hole at the center, which may serve as molecular models for the monolayer boron α sheet. Chemical bonding analysis indicates that B_{36} and B_{36}^- are all-boron analogues of coronene ($C_{24}H_{12}$), featuring concentric dual π aromaticity with an inner π sextet and an outer π sextet. The hydrogenated $B_{36}H_6$ (C_{6v}, $^1A_1$) model cluster shows similar bonding properties, which possesses concentric triple aromaticity with inner π, outer π, and outer σ sextets.

1. Introduction

Over the past decade, elemental boron clusters[1–9] and relevant low-dimensional nanostructures (fullerenes, monolayer-sheets, nanotubes, *etc.*)[10–15] have been intriguing molecular and/or nanoscale systems of interest, for which the elucidation of structures and bonding is a central focus. In particular, recent combined experimental and theoretical studies have led to a systematic understanding of the structural and bonding properties of small boron clusters,[5–9] uncovering a flat land of boron that is in stark contrast to bulk boron and boron alloys, in which three-dimensional (3D) structural units dominate. Planar (2D) or quasi-planar boron clusters were established up to $n = 16$ for cationic B_n^+ clusters.[1] For B_n^- anion clusters, the 2D structures were shown to exist at least up to $n = 24$, with the upper limit remaining open.[9] The critical size of 2D-to-3D transition for neutral B_n clusters is generally believed to be at around $n = 20$,[7] hinting that it is quite unlikely to observe 2D neutral B_n clusters at $n > 20$. The planarity or quasi-planarity of boron clusters is attributed to their nature of electron deficiency, which leads to (π and σ) aromaticity and antiaromaticity.[5,6,8,16–21] However, definitive structural information on $B_n^+/B_n/B_n^-$ clusters beyond $n = 24$ has remained rather elusive.[22,23]

In the current contribution, we report on computational evidence for the quasi-planar all-boron aromatic clusters: B_{36} (C_{6v}, $^1A_1$) and B_{36}^- (C_{2v}, $^2A_1$). These global-minimum clusters were obtained *via* Stochastic Surface Walking (SSW) structural searches[24] and the energetics evaluated using the validated density-functional theory (DFT) method at the PBE0/6-311+G* level.[25–27] The B_{36} and B_{36}^- clusters feature 2D close-packing of boron with a perfect hexagonal hole at the center, which should serve as valuable molecular models for the monolayer boron α sheet.[10,11,28] Bonding analysis indicates that they possess concentric dual π aromaticity, where one set of six π electrons is delocalized around the inner B_6 ring and another sextet is globally delocalized in the outer B_{30} double-chain ribbon. This π bonding pattern is in close analogy to that of coronene ($C_{24}H_{12}$), the latter being developed in the pioneering work reported by Boldyrev and coworkers.[29] The B_{36} and B_{36}^- species represent a record size for free-standing, planar or quasi-planar atomic clusters. During the preparation of this manuscript, a paper on the similar topic by Li, Wang, and coworkers[22] appeared, which reached the same global-minimum structures for B_{36} and B_{36}^- using the Cartesian Walking and Basin Hopping structural searches. The current work and that of ref. 22 are independent of each other.

2. Computational methods

Global-minimum structural searches were carried out using the SSW algorithm, aided with extensive manual structural

[a] *Nanocluster Laboratory, Institute of Molecular Science, Shanxi University, Taiyuan 030006, China. E-mail: hj.zhai@sxu.edu.cn, lisidian@sxu.edu.cn*
[b] *Department of Chemistry, Fudan University, Shanghai 200433, China*
[c] *State Key Laboratory of Quantum Optics and Quantum Optics Devices, Shanxi University, Taiyuan 030006, China*

† Electronic supplementary information (ESI) available: Alternative optimized structures of B_{36} and B_{36}^- (Fig. S1 and S2); detailed structures of B_{36}/B_{36}^- and $B_{36}H_6/B_{36}H_6^-$ at the PBE0 level with bond distances (Fig. S3 and S4); and comparisons of the π canonical molecular orbitals of B_{36}, $B_{36}H_6$, and coronene ($C_{24}H_{12}$) (Fig. S5). See DOI: 10.1039/c4cp02032d

constructions as well. The SSW method has been previously utilized to search for the global minimum of clusters with complex potential energy surfaces, such as short-ranged Morse clusters and carbon clusters up to 100 atoms.[30] Subsequently, the relative energies of the identified low-lying structures were fully optimized using DFT at the hybrid PBE0/6-311+G* level,[25–27] which was lately benchmarked as a reliable DFT method for the boron system, in particular in terms of energetics.[15,31] The lowest-lying ten isomers are also optimized at the meta-generalized TPSSh level.[32] Frequency calculations were performed to ensure that the reported structures are true minima. All PBE0 and TPSSh structural optimizations, frequency analyses, and electronic structure calculations were accomplished using the Gaussian 09 package.[33]

3. Results and discussion

3.1. Structures

The global-minimum and representative low-lying structures of B_{36} (**1–4**) and B_{36}^- (**5–8**) at the PBE0/6-311+G* level are depicted in Fig. 1, along with their hydrogenated $B_{36}H_6$ (**9**) and $B_{36}H_6^-$ (**10**) model clusters. Alternative optimized structures of B_{36} and B_{36}^- are shown in Fig. S1 and S2 in the ESI;† detailed structural information on **1**, **5**, **9**, and **10**, including their bond distances, is shown in Fig. S3 and S4 in the ESI.† The energetics at the PBE0 and TPSSh levels are highly consistent with each other, and only PBE0 data will be discussed below. It is immediately apparent that the quasi-planar, circular **1** and **5** species are the global-minimum structures, which are independent of and confirm those of Li, Wang, and coworkers.[22] The neutral B_{36} (**1**, C_{6v}, $^1A_1$) global minimum is particularly well defined on the potential energy surface, with alternative structures being at least ~1.1 eV higher in energy. The much sought low-dimensional boron nanostructures,[10–15] such as tubular triple-rings (**2** and **6**), double-rings (**3** and **7**), and cage-like fullerenes (**4** and **8**), are also true minima on the potential energy surfaces, but these are energetically unfavorable. Note that prior computational studies have proposed candidate structures for the B_{36} cluster, including structure **1**,[34] but no global-minimum searches have been performed except for ref. 22, to our knowledge.

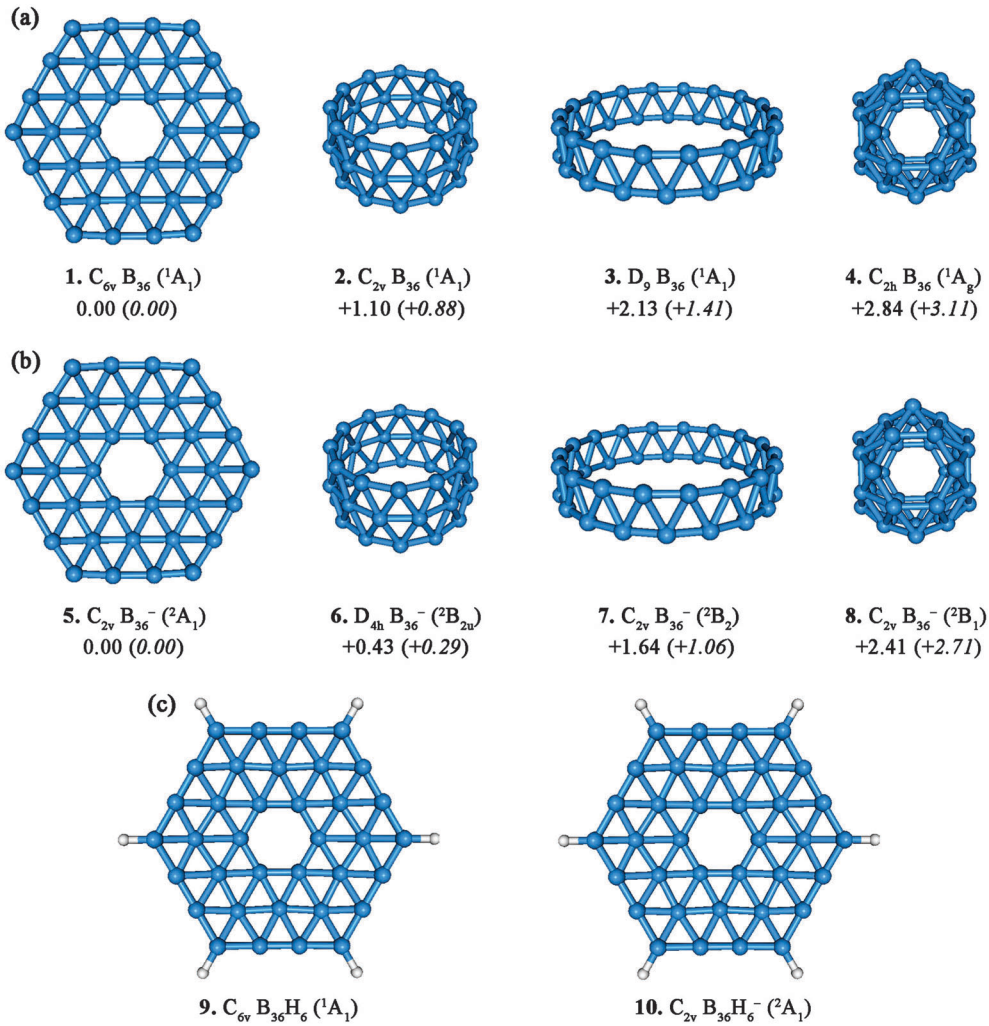

Fig. 1 Selected optimized structures at the PBE0/6-311+G* level for B_{36} (**1–4**), B_{36}^- (**5–8**), and their hydrogenated clusters $B_{36}H_6$ (**9**) and $B_{36}H_6^-$ (**10**). The B_{36} (**1**) and B_{36}^- (**5**) structures are established as the global minima. Relative energies are shown in eV at the PBE0 and TPSSh (in *italic*) levels.

Structures **1** and **5** adopt a quasi-planar and circular shape, with a hexagonal hole positioning at the center. These may be viewed alternatively as composed of three concentric B rings: the inner B_6 ring, the middle B_{12} ring, and the outer B_{18} ring. The B atoms are in-plane tri-, tetra-, penta-, or hexacoordinated, leading to electron deficiency for the systems, in particular for the middle B_{12} ring with pure hexacoordinate B centers. Notably, the configurational energy spectra of B_{36} and B_{36}^- are dominated by 2D structures (Fig. S1 and S2 in ESI†). For example, eight out of thirteen low-lying B_{36} structures within ~2 eV above the global minimum are 2D, whereas thirteen out of twenty low-lying B_{36}^- structures within ~2 eV are 2D. This potency to adopt 2D geometries at such a large size is probably unique to boron clusters.

3.2. Chemical bonding: concentric dual π aromaticity and analogy to coronene

The chemical bonding pattern in the global-minimum **1** and **5** clusters, as revealed from the adaptive natural density partitioning (AdNDP) analysis,[35] is intriguing. AdNDP represents the bonding of a molecule in terms of *n*-center two-electron (*n*c-2e) bonds, with *n* ranging from one to the total number of atoms in the molecule. The AdNDP analysis thus recovers the classical Lewis bonding elements (lone pairs and 2c-2e bonds), as well as the nonclassical, delocalized *n*c-2e bonds. As depicted in Fig. 2a, of the 54 pairs of valence electrons in B_{36} (**1**), there are 18 peripheral 2c-2e σ bonds for the outer ring, as well as six delocalized 3c-2e σ bonds around the inner ring. The σ bonding between the inner and outer rings is accomplished by eighteen delocalized 4c-2e σ bonds, among which twelve link the outer and middle rings and six link the middle and inner rings. Note that, although only delocalized over small B_3 or B_4 "islands", the 3c-2e and 4c-2e σ bonds cover the whole boron sheet almost evenly. Overall, the σ framework consumes 42 pairs of electrons.

The remaining 12 pairs of electrons in **1** are responsible for the π bonding, in which the six 4c-2e π bonds form islands around the six corners on the sheet. Of the more delocalized π bonds, three are 12c-2e bonds mainly delocalized around the central B_6 ring; while three 36c-2e bonds are responsible for π bonding between the middle and outer rings, being mainly delocalized on the B_{30} double-chain ribbon. Remarkably, these three 12c-2e and three 36c-2e π bonds are responsible for the global, delocalized π bonding in the boron sheet, forming a concentric dual π aromatic system, whose inner and outer sets of bonds both conform to the $(4n + 2)$ Hückel rule for aromaticity. The bonding nature of **5** is essentially the same, except that an extra electron occupies the lowest unoccupied molecular orbital of **1**. We believe that concentric dual π aromaticity holds the key to understanding the structure and stability of quasi-planar **1** and **5** clusters. It is noted that our understanding of the nature of the global π bonding in **1** and **5** differs somewhat from that in ref. 22.[36]

Since a rhombic 4c-2e bond (and to a less extent, a 3c-2e or 5c-2e bond), either π or σ, in the double-chain boron nanoribbon systems is basically equivalent to a 2c-2e C–C bond in the hydrocarbons,[31,37–39] a close connection between **1** (Fig. 2a) and coronene ($C_{24}H_{12}$; Fig. 2c)[29] is readily established, making **1** an all-boron analog of coronene.[36] To be specific, the three 12c-2e π bonds associated with the inner B_6 ring in **1** (Fig. 2a; the third row) show exact one-to-one correspondence to the three 6c-2e π bonds in coronene (Fig. 2c). The three 36-2e π bonds in **1** (Fig. 2a; the second row) are identical to the three 24c-2e π bonds in coronene, whereas the six 4c-2e island π bonds in **1** (Fig. 2a; the second row) are equivalent to the six 2c-2e C–C π bonds in coronene. This analogy can also be revealed from the π canonical molecular orbitals (CMOs). As shown in

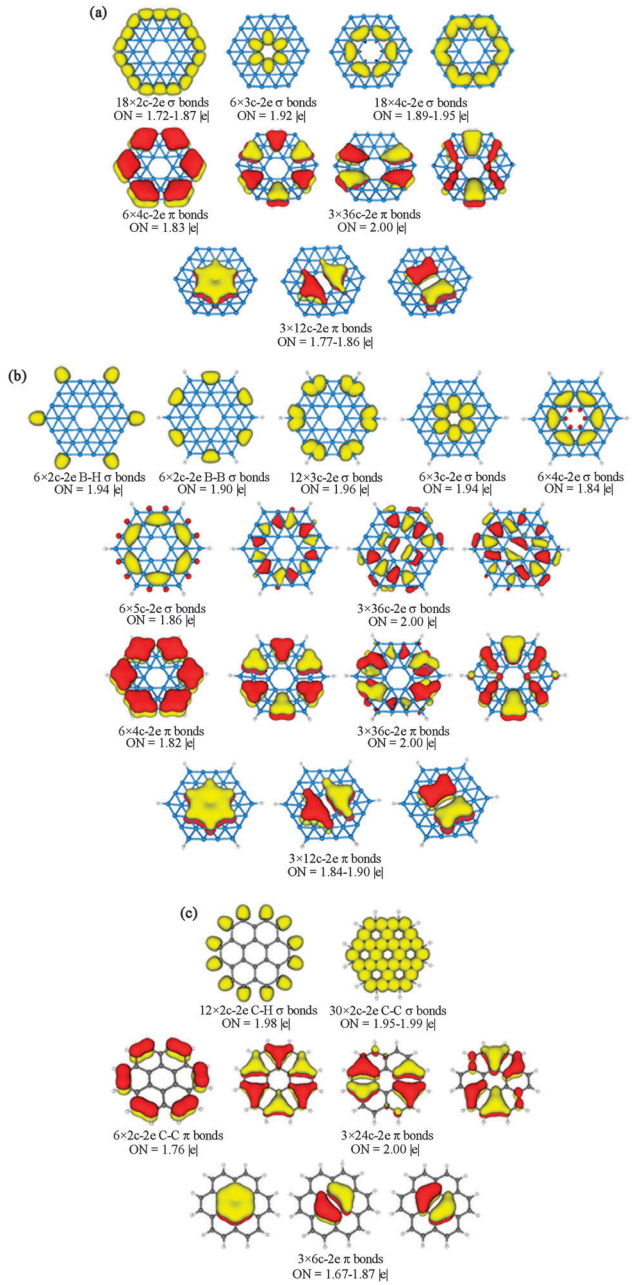

Fig. 2 Bonding patterns as revealed from the adaptive natural density partitioning (AdNDP) analyses of (a) B_{36} (**1**) and (b) $B_{36}H_6$ (**9**), as compared to (c) coronene ($C_{24}H_{12}$). The occupation numbers (ONs) are indicated.

Fig. S5 in the ESI,† the twelve π CMOs of B_{36} (**1**) show a one-to-one correspondence with those of D_{6h} $C_{24}H_{12}$. Inorganic molecular systems with concentric π aromaticity have been very rare and only a few examples (B_{13}^+, B_{19}^-, and $C_3B_9^{3+}/C_5B_{11}^+$)[8,40,41] are known, among which $C_3B_9^{3+}/C_5B_{11}^+$ are pure model clusters and experimentally not viable because they are not the global minima.[41]

Herein it is also of interest to comment on the cage-like fullerene structures: B_{36} (**4**) and B_{36}^- (**8**). These can be constructed from eight triangular, quasi-planar B_6 units, each sharing a corner with three neighboring B_6 units. As a consequence, six hexagonal holes are generated on the surface of a spherical cage: one on top, one at the bottom, and four on the waist. Alternatively, **4** and **8** can be built upon twelve interwoven B_9 double-chain ribbons, which have been recognized lately as robust building blocks for low-dimensional boron nanomaterials. Every B atom is on the edge of a hexagonal hole. Two of the B atoms around a hexagonal hole are tetracoordinated, as compared to four that are pentacoordinated. Overall, twelve B atoms in **4** or **8** are tetracoordinated and twenty-four are pentacoordinated, where the former atoms pop out slightly from the sphere. Structurally, these appear to be ideal candidates for all-boron fullerenes. However, they turn out to be at least ~2 eV above the quasi-planar global minima **1** and **5** (Fig. 1). Strains due to the curvature of the cage may partly account for the instability of **4** or **8**. However, we believe that the electron counting also plays a key role. Preliminary bonding analysis of **4** suggests that, of the 54 pairs of valence electrons, 44 pairs can be located as 3c-2e σ bonds, one for every B_3 triangles on the sphere. The σ framework in **4** thus appears to be perfect. On the other hand, the π framework possesses 10 pairs of electrons, which is clearly less than ideal. Considering the cluster geometry, either 8 or 12 pairs of π electrons would better cover the cage, smoothly and evenly. This understanding should help design appropriate all-boron fullerenes.

3.3. Chemical bonding in hydrogenated $B_{36}H_6$ and $B_{36}H_6^-$ model clusters

As a preliminary exploration, we also constructed the hydrogenated $B_{36}H_6$ (**9**, C_{6v}, $^1A_1$) and $B_{36}H_6^-$ (**10**, C_{2v}, $^2A_1$) model clusters, as shown in Fig. 1c. These structures represent true minima on their potential energy surfaces. Interestingly, hydrogenation appears to enhance the planarity of the boron sheet in **9** with respect to **1**, which can be attributed to the slightly expanded size of the outer B_{18} ring upon hydrogenation.

In terms of the AdNDP bonding pattern, the π framework in $B_{36}H_6$ (**9**) (Fig. 2b; the bottom two rows) is identical to that in B_{36} (**1**), as are the six 3c-2e and six 4c-2e σ bonds associated with the inner B_6 ring (Fig. 2b; top row). The 18 peripheral σ bonds in the outer ring (Fig. 2b; top row) are essentially maintained, except that twelve of them are transformed into 3c-2e σ bonds. Major changes occur with the σ bonds that connect the outer and middle rings. There are twelve such 4c-2e σ bonds in **1** that are located near the apex B atoms. In **9**, only six of these maintain as islands, but shift to edge positions and slightly expand as 5c-2e σ bonds, whereas the remaining three σ bonds become completely delocalized (Fig. 2b; second row). It is stressed that the nine σ bonds associated with the middle and outer rings in **9** are closely parallel to the nine π bonds (Fig. 2b; the second *versus* third row), suggesting both π and σ aromaticity. Thus, hydrogenation produces unique clusters **9** and **10**, whose inner π, outer π, and outer σ sextets each conform to the $(4n + 2)$ Hückel rule for aromaticity, collectively rendering concentric triple aromaticity to these hydroboron clusters. As demonstrated in Fig. S5 in the ESI,† the twelve π CMOs of $B_{36}H_6$ (**9**) are similar to those in **1** and $C_{24}H_{12}$, making **9** (and **10**) the first boron hydride analogues of coronene.

3.4. Simulated photoelectron spectra

To aid experimental characterization of the global-minimum B_{36} (**1**, C_{6v}, $^1A_1$) and B_{36}^- (**5**, C_{2v}, $^2A_1$) clusters, we calculated the ground-state adiabatic and vertical detachment energies (ADEs and VDEs) of **5** at the PBE0/6-311+G* level, calculated its VDEs for the excited-state transitions at the time-dependent DFT (TDDFT) level,[42] and simulated its photoelectron spectrum as shown in Fig. 3a. The spectrum shows well-structured features with the ground-state ADE/VDE values of 3.11/3.15 eV and an energy gap of 0.84 eV, the latter being characteristic of a stable, closed-shell neutral cluster. The simulated spectrum (Fig. 3a) agrees well with the recent experimental data.[22] For example, first two VDEs are measured to be 3.3 ± 0.1 and 4.08 ± 0.03 eV, respectively, as compared to the calculated values of 3.15 and 3.99 eV. We also simulated the photoelectron spectrum of $B_{36}H_6^-$ (**10**) (Fig. 3b), whose first two bands (ADE/VDE: 2.95/3.30 eV; energy gap: 0.77 eV)

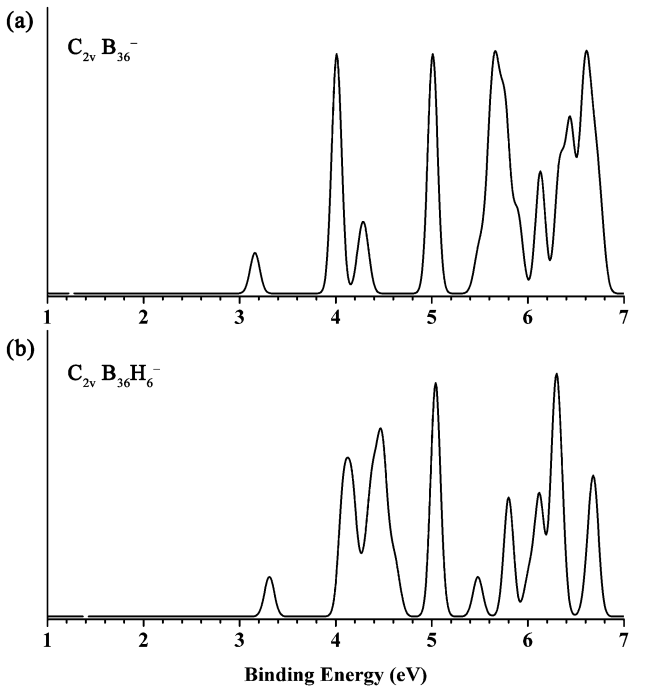

Fig. 3 Simulated photoelectron spectra of B_{36}^- (**5**) and (b) $B_{36}H_6^-$ (**10**) based on the PBE0/6-311+G* and TDDFT calculations. The simulations were done by fitting the distribution of calculated vertical detachment energies with unit-area Gaussian functions of 0.1 eV half-width.

are remarkably similar to those of **5**, consistent with their similarities in frontier CMOs.

4. Conclusions

In conclusion, the structural and bonding properties of B_{36} and B_{36}^- clusters are studied *via* extensive global-minimum searches and density-functional calculations. Quasi-planar, circular, close-packing structures with a central hexagonal hole are established as the global minima for both species, in line with the findings in a recent work reported by Li, Wang, and coworkers.[22] Chemical bonding analysis reveals concentric dual π aromaticity in the species, akin to coronene. The current results represent a record size to date for a planar or a quasi-planar atomic cluster, suggesting that the notion of the 2D-to-3D transition for B_n neutral clusters occurring at around $n = 20$ needs to be updated[7] and that there appears to be much room to explore for planar or quasi-planar B_n and B_n^- clusters. Furthermore, hydrogenated quasi-planar $B_{36}H_6$ and $B_{36}H_6^-$ model clusters are also true minima with inner π, outer π, and outer σ sextets, collectively leading to concentric triple aromaticity.

Note added at proof

A very recent paper by the current authors[43] reported the observation of the first all-boron fullerenes or borospherenes, B_{40}^- and B_{40}. The B_{40}^- anion cluster has a coexisting quasi-planar isomer.

Acknowledgements

This work was supported by the National Natural Science Foundation of China (21243004, 21373130, 21173051, and 21361130019), the Shanxi International Cooperation project (201308018), the 973 program (2011CB808500 and 2013CB834603), and in part by the State Key Laboratory of Quantum Optics and Quantum Optics Devices (KF201402). H.J.Z. gratefully acknowledges the start-up fund from Shanxi University for support.

References

1 E. Oger, N. R. M. Crawford, R. Kelting, P. Weis, M. M. Kappes and R. Ahlrichs, *Angew. Chem., Int. Ed.*, 2007, **46**, 8503.
2 I. Boustani, *Phys. Rev. B: Condens. Matter Mater. Phys.*, 1997, **55**, 16426.
3 J. E. Fowler and J. M. Ugalde, *J. Phys. Chem. A*, 2000, **104**, 397.
4 J. I. Aihara, H. Kanno and T. Ishida, *J. Am. Chem. Soc.*, 2005, **127**, 13324.
5 H. J. Zhai, A. N. Alexandrova, K. A. Birch, A. I. Boldyrev and L. S. Wang, *Angew. Chem., Int. Ed.*, 2003, **42**, 6004.
6 H. J. Zhai, B. Kiran, J. Li and L. S. Wang, *Nat. Mater.*, 2003, **2**, 827.
7 B. Kiran, S. Bulusu, H. J. Zhai, S. Yoo, X. C. Zeng and L. S. Wang, *Proc. Natl. Acad. Sci. U. S. A.*, 2005, **102**, 961.
8 W. Huang, A. P. Sergeeva, H. J. Zhai, B. B. Averkiev, L. S. Wang and A. I. Boldyrev, *Nat. Chem.*, 2010, **2**, 202.
9 I. A. Popov, Z. A. Piazza, W. L. Li, L. S. Wang and A. I. Boldyrev, *J. Chem. Phys.*, 2013, **139**, 144307.
10 X. B. Yang, Y. Ding and J. Ni, *Phys. Rev. B: Condens. Matter Mater. Phys.*, 2008, **77**, 041402(R).
11 H. Tang and S. Ismail-Beigi, *Phys. Rev. Lett.*, 2007, **99**, 115501.
12 N. G. Szwacki, A. Sadrzadeh and B. I. Yakobson, *Phys. Rev. Lett.*, 2007, **98**, 166804.
13 D. L. V. K. Prasad and E. D. Jemmis, *Phys. Rev. Lett.*, 2008, **100**, 165504.
14 S. De, A. Willand, M. Amsler, P. Pochet, L. Genovese and S. Goedecker, *Phys. Rev. Lett.*, 2011, **106**, 225502.
15 F. Y. Li, P. Jin, D. E. Jiang, L. Wang, S. B. B. Zhang, J. J. Zhao and Z. F. Chen, *J. Chem. Phys.*, 2012, **136**, 074302.
16 A. N. Alexandrova, A. I. Boldyrev, H. J. Zhai and L. S. Wang, *Coord. Chem. Rev.*, 2006, **250**, 2811.
17 D. Yu. Zubarev and A. I. Boldyrev, *J. Comput. Chem.*, 2007, **28**, 251.
18 A. P. Sergeeva, D. Yu. Zubarev, H. J. Zhai, A. I. Boldyrev and L. S. Wang, *J. Am. Chem. Soc.*, 2008, **130**, 7244.
19 A. P. Sergeeva, B. B. Averkiev, H. J. Zhai, A. I. Boldyrev and L. S. Wang, *J. Chem. Phys.*, 2011, **134**, 224304.
20 Z. A. Piazza, W. L. Li, C. Romanescu, A. P. Sergeeva, L. S. Wang and A. I. Boldyrev, *J. Chem. Phys.*, 2012, **136**, 104310.
21 A. P. Sergeeva, Z. A. Piazza, C. Romanescu, W. L. Li, A. I. Boldyrev and L. S. Wang, *J. Am. Chem. Soc.*, 2012, **134**, 18065.
22 Z. A. Piazza, H. S. Hu, W. L. Li, Y. F. Zhao, J. Li and L. S. Wang, *Nat. Commun.*, 2014, **5**, 3113.
23 W. L. Li, Y. F. Zhao, H. S. Hu, J. Li and L. S. Wang, *Angew. Chem., Int. Ed.*, 2014, **53**, 5540.
24 C. Shang and Z. P. Liu, *J. Chem. Theory Comput.*, 2013, **9**, 1838.
25 J. P. Perdew, K. Burke and M. Ernzerhof, *Phys. Rev. Lett.*, 1996, **77**, 3865.
26 J. P. Perdew, K. Burke and M. Ernzerhof, *Phys. Rev. Lett.*, 1997, **78**, 1396.
27 C. Adamo and V. Barone, *J. Chem. Phys.*, 1999, **110**, 6158.
28 T. R. Galeev, Q. Chen, J. C. Guo, H. Bai, C. Q. Miao, H. G. Lu, A. P. Sergeeva, S. D. Li and A. I. Boldyrev, *Phys. Chem. Chem. Phys.*, 2011, **13**, 11575.
29 D. Yu. Zubarev and A. I. Boldyrev, *J. Org. Chem.*, 2008, **73**, 9251.
30 X. J. Zhang, C. Shang and Z. P. Liu, *J. Chem. Theory Comput.*, 2013, **9**, 3252.
31 H. Bai, Q. Chen, C. Q. Miao, Y. W. Mu, Y. B. Wu, H. G. Lu, H. J. Zhai and S. D. Li, *Phys. Chem. Chem. Phys.*, 2013, **15**, 18872.
32 J. Tao, J. P. Perdew, V. N. Staroverov and G. E. Scuseria, *Phys. Rev. Lett.*, 2003, **91**, 146401.
33 M. J. Frisch, *et al.*, *Gaussian 09, revision D.01*, Gaussian, Inc., Wallingford, CT, 2009.
34 F. Y. Tian and Y. X. Wang, *J. Chem. Phys.*, 2008, **129**, 024903.

35 D. Yu. Zubarev and A. I. Boldyrev, *Phys. Chem. Chem. Phys.*, 2008, **10**, 5207.
36 The concentric dual π bonding pattern in **1** and **5** is clear. The inner B ring contributes little to the three 36c-2e π bonds, whereas the contribution of the outer B ring to the three 12c-2e π bonds is small (7–12%; see Fig. 2a). Furthermore, the analogy of **1** and **5** to coronene ($C_{24}H_{12}$) offers critical insight, which helps rationalize the stability and the nature of bonding in **1** and **5**. These ideas have not been discussed in the literature.
37 H. J. Zhai, Q. Chen, H. Bai, H. G. Lu, W. L. Li, S. D. Li and L. S. Wang, *J. Chem. Phys.*, 2013, **139**, 174301.
38 D. Z. Li, Q. Chen, Y. B. Wu, H. G. Lu and S. D. Li, *Phys. Chem. Chem. Phys.*, 2012, **14**, 14769.
39 W. L. Li, C. Romanescu, T. Jian and L. S. Wang, *J. Am. Chem. Soc.*, 2012, **134**, 13228.
40 G. Martinez-Guajardo, A. P. Sergeeva, A. I. Boldyrev, T. Heine, J. M. Ugalde and G. Merino, *Chem. Commun.*, 2011, **47**, 6242.
41 S. Erhardt, G. Frenking, Z. Chen and P. V. R. Schleyer, *Angew. Chem., Int. Ed.*, 2005, **44**, 1078.
42 R. Bauernschmitt and R. Ahlrichs, *Chem. Phys. Lett.*, 1996, **256**, 454.
43 H. J. Zhai, Y. F. Zhao, W. L. Li, Q. Chen, H. Bai, H. S. Hu, Z. A. Piazza, W. J. Tian, H. G. Lu, Y. B. Wu, Y. W. Mu, G. F. Wei, Z. P. Liu, J. Li, S. D. Li and L. S. Wang, *Nat. Chem.*, 2014, DOI: 10.1038/NCHEM.1999.